Effects of the Plasma Blob Nonlinear Formation/Transport on Impurity Transport in the SOL Regions*)

Tomoyuki MAEDA, Hiroki HASEGAWA[1,2)], Seiji ISHIGURO[1,2)], Kazuo HOSHINO and Akiyoshi HATAYAMA

Graduate School of Science and Technology, Keio University, Yokohama 223-8522, Japan
[1)]*National Institute for Fusion Science (NIFS), National Institutes of Natural Sciences (NINS), Toki 509-5292, Japan*
[2)]*Department of Fusion Science, SOKENDAI (The Graduate University for Advanced Studies), Toki 509-5292, Japan*

(Received 28 December 2018 / Accepted 6 May 2019)

The purpose of this study is to make clear the effects of the plasma blob on the impurity transport in the Scrape-Off Layer (SOL) regions. By using the two-dimensional (2D) interchange turbulence model with plasma transport along magnetic field line, we have simulated the plasma blob formation and transport in the SOL regions. We have studied the effects of the plasma blob on the impurity transport by using impurity equations of motion in the trace impurity limit. The results show that the plasma blob transport direction is not only the radial direction but also poloidal direction due to the plasma transport along the magnetic field line. Also, the impurity ions are transported radially outward with the plasma blob transport and the velocity of the impurity ions transport is the same order to the plasma blob velocity radially outward. These results implied that the impurity transport with the plasma blob may possibly be not only diffusion but also convection. Moreover, this motion of the impurity ions seems like eddy motion. As a next step, we study relation between this eddy motion of impurity ions and the plasma blob motion. That is our future work.

Keywords: plasma blob, non-diffusion, two-dimensional interchange turbulence model, impurity transport, test particle model

DOI: 10.1585/pfr.14.3403133

1. Introduction

Understanding the impurity transport is one of the most important issues for realization of future fusion reactors. Many experimental and theoretical studies have been done in order to understand and control the impurity transport in the SOL background plasmas.

Recent studies have shown that non-diffusive radial transport is important for undestanding the plasma density distribution and impurity ions transport in the SOL regions [1–6]. In some devices, the plasma blob has been observed experimentally [6–8]. However, the formation mechanism of the plasma blob has not yet been understood well. Also, the effect of the plasma blob on the impurity transport is not clear. Most of the plasma blob studies mainly focus on the plasma blob transport. In these studies, plasma density like a plasma blob is given as initial condition and then the plasma blob transport is only simulated numerically. There are several studies simulating the plasma blob based on the 2D interchange turbulence model [1–6]. In these previous studies, effects of blob on impurity transport were not studied. In recent study using 3D PIC simulation [9–12], effects of blob on impurity transport have been extensively studied, but plasma blob formation process has not been simulated, but simply treated as an initial plasma potential perturbation. In our study, not only the plasma blob transport process, but also its formation process has been simulated without giving the initial plasma density like a plasma blob. We have simulated by using the initial plasma density which has density gradient radially in the SOL regions. In section2, the initial condition will be explained in detail.

Final target of our study is to make clear the effects of the plasma blob on the impurity transport in the SOL regions of fusion devices. As a first step, we focused on the plasma blob formation caused by edge turbulence by applying partially linearized version of two-dimensional (2D) interchange turbulence model without plasma transport along magnetic field line to the SOL regions in Ref. [13]. This model consists of the density and vorticity equations with $\mathbf{E}\times\mathbf{B}$ drift and curvature drift. The effects of the plasma blob on the impurity transport have been studied by using a simple test particle model of impurities with their equations of motion. The equations of impurity motion have been solved and test impurity trajectories are followed by taking into account the background plasma potential structure provided by the 2D interchange turbulence model in the trace impurity limit. The results showed that a blob was produced by the interchange instability and trans-

author's e-mail: maeda@ppl.appi.keio.ac.jp

*) This article is based on the presentation at the 27th International Toki Conference (ITC27) & the 13th Asia Pacific Plasma Theory Conference (APPTC2018).

ported radially towards the wall by $\mathbf{E}\times\mathbf{B}$ drift. Also, impurity ions were transported by $\mathbf{E}\times\mathbf{B}$ drift around the plasma blob. As a second step, in this paper, we have considered the following factor; plasma transport along magnetic field line with sheath effects on the divertor plates, to simulate more similar to actual plasma density and potential condition as background plasma of impurity transport. The effects of the plasma blob on the impurity transport have been studied by using the equations of impurity motion as in the same manner as the method in the Ref. [13]. Moreover, we have compared the plasma blob velocity with impurity ions velocity and considered the time evolution of impurity ions ensemble mean of dispersion in order to understand the effects of the plasma blob on the impurity transport.

In section 2, we will explain the 2D interchange turbulence model shortly. Also, test particle model of the impurity transport will be explained. In section 3, the simulation results of the plasma blob formation and transport will be shown. Also, its effects on the impurity transport will be described with the simulation results and analyses. The summary and the future work will be given in section 4.

2. Numerical Model

2.1 Plasma blob model

In this paper, the plasma blob formation and transport are simulated by using the 2D interchange turbulence model [14–16]. This model has two basic equations; the density equation and the vorticity equation. Assuming the iso-thermal approximation, the equations are shown as,

$$\left(\frac{\partial}{\partial t}+\mathbf{v_E}\cdot\nabla_\perp\right)n+g\left(\frac{\partial n}{\partial y}-\frac{\partial\phi}{\partial y}\right)-D\nabla_\perp^2 n=\sigma_1, \quad (1)$$

$$\left(\frac{\partial}{\partial t}+\mathbf{v_E}\cdot\nabla_\perp\right)\nabla_\perp^2\phi+g\frac{\partial n}{\partial y}-\nu\nabla_\perp^4\phi=\sigma_2, \quad (2)$$

where n, ϕ and t are the normalized plasma density, potential and time, respectively. They are normalized as follows: $n\sim n/n_0$, $\phi\sim e\phi/T_e$, $t\sim\Omega_i t$, where n_0, e, T_e and Ω_i are the reference density, unit charge, electron temperature and ion cyclotron frequency, respectively. The reference density represents the background plasma density on the Separatrix. In Eqs. (1) and (2), $\nabla_\perp=\hat{\mathbf{x}}(\partial/\partial\mathbf{x})+\hat{\mathbf{y}}(\partial/\partial\mathbf{y})$, $\mathbf{v_E}=(\mathbf{E}\times\mathbf{B})/B^2$, $\mathbf{E}$ is the electric field, and $\mathbf{B}$ is the magnetic field. Here, we assume the uniform troidal magnetic field to deal with magnetic field simply. In this study, we have solved the equations in a simple 2D slab geometry as shown in Fig. 1. L_x and L_y are the system size in the x and y directions, respectively. The coordinates x and y are normalized by ρ_s correspond to the radial and poloidal directions, respectively. The symbol ρ_s is ion Larmor radius given by $\rho_s=c_s/\Omega_i$, where c_s is the ion acoustic speed given by $c_s=\sqrt{T_e/m_i}$, m_i is the ion mass. Here, we reflect curvature magnetic field effect in parameter g. The parameter g is the magnetic curvature-induced gravity defined by $g\equiv(2\rho_s)/R$, R is the major radius. This parameter is important for the plasma blob formation, because the gravity force direction is in the opposite direction to the plasma density gradient direction. Therefore, the interchange instability appears due to the parameter g. The parameters D and ν is the normalized diffusion coefficient and viscosity coefficient, respectively. To drive Eqs. (1) and (2), we have assumed quasi-neutrality and used current continuity equation ($\nabla\cdot\mathbf{J}=0$) to take into account the effect of parallel current along the magnetic field line. The factor σ_1 and σ_2 represent the plasma transport along the magnetic field line given by $\sigma_1=-\alpha n\exp[-\phi]$, $\sigma_2=\alpha(1-\exp[-\phi])$, where α is the parallel sheath conductivity defined $\alpha\equiv(2\rho_s)/L_\parallel$, $L_\parallel$ is parallel connection length of the magnetic field line. The factor α measures the net parallel current into the divertor plates [16]. These factors (σ_1, σ_2) are derived from 1D sheath model in parallel to the magnetic field line. The plasma blob is connected to divertor plates through sheath regions in front of divertor plates. Induced polarization electric field in the plasma blob is remained due to this connection. Therefore, it is necessary to consider this effect for the plasma blob simulation. The forth term in L.H.S. of Eq. (1) represents the effect of $\mathbf{E}\times\mathbf{B}$ drift. The third term in L.H.S. of Eqs. (1) and (2) represent the effect of magnetic curvature drift.

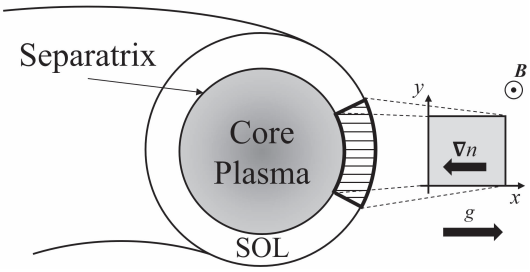

Fig. 1 Schematic drawing of the computational domain. Simple 2D slab geometry is adopted to simulate the outer SOL region.

In this paper, the input parameters are as follows. These are $D=0.01$, $\nu=0.01$, $T_e=50\,\mathrm{eV}$, $g=8.0\times10^{-4}$, $\alpha=3.0\times10^{-5}$. These parameters are based on typical tokamak SOL parameters [14, 16]. The computational domain size for the simulation is set as $L_x=L_y=100$. The time integration is performed by fourth-order Runge-Kutta method. The second terms in L.H.S. of Eqs. (1) and (2) are calculated using Arakawa-Jacobian method. The others are using central-difference method. The following Dirichlet boundary conditions are adopted for this simulation,

$$n(0,y)=1, n(L_x,y)=0, n(x,0)=n(x,L_y),$$
$$\phi(0,y)=0, \phi(L_x,y)=0, \phi(x,0)=\phi(x,L_y).$$

The initial plasma density is given by exponential distribution,

$$n(x,y)=n_0\exp\left(-\frac{9x}{200}\right). \quad (3)$$

The initial plasma potential fluctuation is given by the following equation,

$$\phi(x,y) = \left(\frac{T_e}{e}\right)\sin\left[\frac{2\pi m y}{L_y}\right]\exp\left[-\frac{\left(x - x_{\rm peak}\right)^2}{100}\right], \quad (4)$$

where m is the wave number in the y direction and $x_{\rm peak}$ is the location of the plasma potential peak in the x direction. In this study, these parameters are set as follows; $m = 5$, $x_{\rm peak} = 20$, and the y direction range of plasma potetial fluctuation is $40 \le y \le 60$. This initial fluctuation provides the plasma blob.

2.2 Impurity model

We have studied the effects of the plasma blob on the impurity transport by using the equations of impurity motion. The equations are given without normalization as

$$m_{\rm imp}\frac{{\rm d}\mathbf{v}}{{\rm d}t} = Ze\left(\mathbf{E} + \mathbf{v}\times\mathbf{B}\right), \quad (5)$$

where $m_{\rm imp}$ is the impurity mass, $\mathbf{v}$ is the velocity of impurity, Z is the valence of impurity, e is the electron charge, $\mathbf{E}$ is the electric field of background plasma, and $\mathbf{B}$ is the magnetic field. In this paper, tungsten (W) impurity with the charge state $Z = 7$ and the mass $m_{\rm imp} = 3.06\times10^{-25}$ kg has been assumed for simplicity. Their initial velocities are set to be the monotonic velocity given by $v = \sqrt{2kT/m_{\rm imp}}$ with T being the same as that of the background plasma temperature ($T = T_e$). Their initial velocities in the x and y direction is given by $v_x = v\sin[2\pi\xi]$, $v_y = v\cos[2\pi\xi]$, where ξ is uniform random number. Totally 10^4 test impurity ions are used in the present simulation. The trajectory of test impurity ions is calculated in real space by using the Buneman-Boris algorithm as in the same manner as the IMPGYRO code [17]. Initially, impurity ions are uniformly loaded in a certain region in the computational domain. In section 3.2, the initial impurity ions distribution will be explained in detail. The main point of this initial impurity distribution is to verify the effects of plasma blob on the impurity transport plainly.

3. Results

In section 3.1, the plasma blob simulation results are shown in two cases. The following two cases of the 2D interchange model have been tried: in Case A plasma transport along magnetic field line is not included ($\alpha = 0$), while in Case B plasma transport along magnetic field line is included ($\alpha = 3.0\times10^{-5}$). These two different models are useful to understand the importance of plasma transport along magnetic field line for plasma blob transport simulation.

In section 3.2, the effects of the plasma blob transport on the impurity transport are shown. As mentioned in Sec. 1 and Sec. 2, the main focus point of this study is making clear of the effects of plasma blob on the impurity transport in the SOL regions. Therefore, the initial impurity profiles are relatively simple and special settings and the plasma blob transport direction is only the radially outward without the effect of plasma trasnport along magnetic field line. In this paper, initial impurity test ions distribution is loaded in the middle of the computational domain. This setting is useful to understand the effects of the plasma blob '*transport*' on the impurity transport. In the previous study by using the 3D PIC simulation [9], the effects of the blob on impurity transport has been considered as the effective radial diffusion coefficients in order to compare that transport with conventional diffusive transports. Then, the effective radial diffusion coefficients in the simulations have been compared with the Bohm diffusion coefficient $D_{\rm B}$ defined as $D_{\rm B} \equiv T_e/(16eB)$. The effective radial diffusion coefficient $D_{{\rm imp}\perp}$ is calculated by $D_{{\rm imp}\perp} = \Gamma_{{\rm imp}\perp}/\nabla_\perp n_{\rm imp}$, where $\Gamma_{{\rm imp}\perp}$ is the impurity ion radial flux on y-z plane at $x = x_{\rm s}$ ($x_{\rm s}$ is the initial boundary of impurity region) and $\nabla_\perp n_{\rm imp}$ is the impurity ions density radial gradient [9]. In this paper, we have considered whether the effects of the plasma blob transport on the impurity transport are convective or not. The initial distributions of plasma density and potential are shown in Fig. 2. Each initial condition is given by Eqs. (3) and (4), respectively.

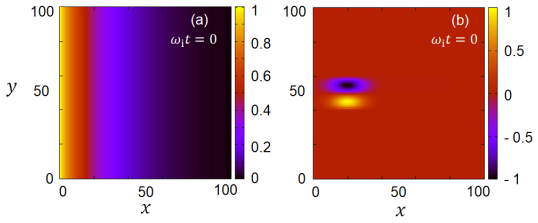

Fig. 2 Initial distribution of (a) plasma density and (b) plasma potential.

3.1 Plasma blob transport

Figures 3 and 4 show the time evolution of the plasma density and potential profiles. Due to the initial plasma potential fluctuation, the plasma region becomes unstable. Rayleigh-Taylor instability has started growing, because the density gradient (∇n) and curvature induced gravity force (g) are in the opposite direction [13]. Then, single blob has been provided. The plasma blob is transported radially outward by the $\mathbf{E}\times\mathbf{B}$ drift. The plasma blob transport in Case B is different from Case A. In Case A, the direction of the plasma blob transport is only $+x$ (= radial outward) direction. In Case B, the direction of the plasma blob transport is $+x$ (= radial outward) and $-y$ (= poloidal) direction. Moreover, there is a difference of the distribution of plasma potential. In Case A, the distribution is symmetry, while in Case B the distribution is asymmetry. Particularly, in Case B the plasma potential on the negative side is lower than the plasma potential positive side.

We have tried to explain these differences by consid-

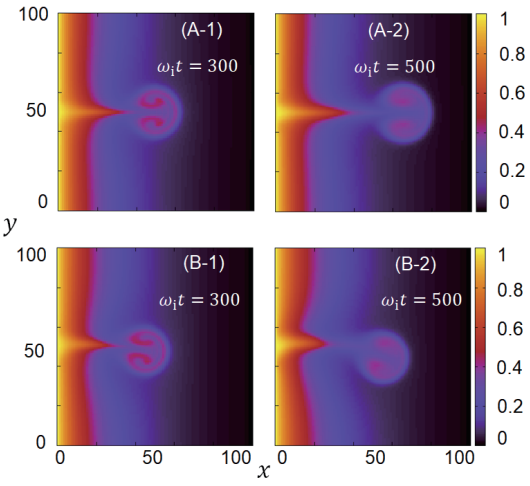

Fig. 3 Simulation results of the time evolution of the plasma density profile in each case. These profiles are shown as a snapshot at various time steps.

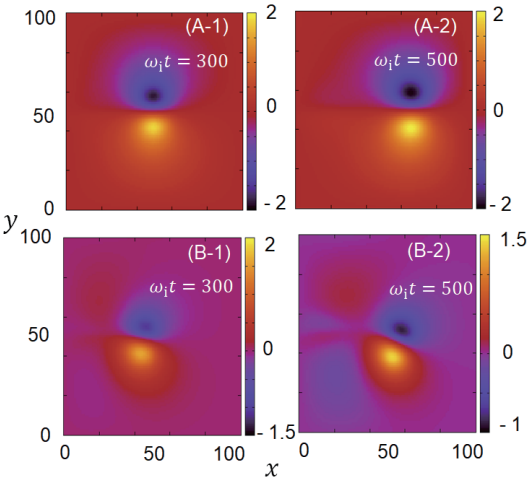

Fig. 4 Simulation results of the time evolution of the plasma potential profile in each case. These profiles are shown as a snapshot at various time steps.

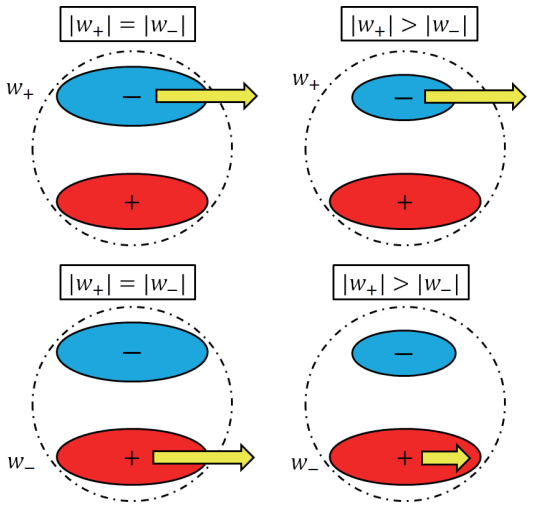

Fig. 5 Schematic drawing of the vorticity in the plasma blob and velocity : (left side) Case A, (right side) Case B. The dash line is the plasma blob edge line. The terms '+' and '-' represent the positive plasma potential and negative plasma potential, respectively. The w_+ and w_- are positive potential side vorticity and positive potential side vorticity, respectively. The arrows represent the velocities given by the vorticities.

ering vorticity. The vorticity is a measure of the rotational spin defined $\mathbf{w} = \nabla \times \mathbf{v}$. In this paper, the velocity $\mathbf{v}$ is given by $\mathbf{v} = \mathbf{v_E} = (\mathbf{E} \times \mathbf{B})/B^2 = (\mathbf{B} \times \nabla\phi)/B^2$. Therefore, the vorticity w is given by $w = \nabla_\perp^2 \phi$. As shown in Fig. 5, there is a difference between positive potential side vorticity (w_+) and negative potential side vorticity (w_-), because plasma potential is asymmetry. The relation between $|w_+|$ and $|w_-|$ is $|w_+| > |w_-|$. Also, the rotation direction of w_+ and w_- are counterclockwise and clockwise direction, respectively. Therefore, velocities provided by each vorticity are different as shown in Fig. 5. The negative side velocity given by w_+ is larger than the positive side velocity given by w_-. Finally, the plasma blob transport direction is $+x$ (= radial outward) and $-y$ (= poloidal) direction.

3.2 Impurity transport by the plasma blob

Figure 6 shows the time evolution of impurity ions distribution. The impurity ions are uniformly distributed in the square region. This square region is set as $40 < x < 60$ and $40 < y < 60$ for understanding the effect of the plasma blob on the impurity transport clearly and avoiding the boundary condition influences on the impurity transport. The plasma blob is generated in the region without impurity ions. Then, the plasma blob is transported radially outward and reached the region where the impurity ions are located. In the First phase, the plasma blob sweeps the impurity ions. In the Next phase, the plasma blob completely penetrates into the impurity regions and the impurity ions are distributed like a ring. Finally, the impurity ions are included in the center of the plasma blob with the plasma blob transport radially outward. The impurity ions are transported by $\mathbf{E} \times \mathbf{B}$ drift around and inside the blob.

In Ref. [9], the 3D PIC model has been developed and the dynamics between impurity ions and plasma blob have been investigated. However, the initial plasma density distribution is set as a gaussian distribution like plasma blob. Moreover, it is difficult to simulate the plasma blob effects on impurity ions transport for a long time-scale because the 3D PIC simulation has high calculation costs.

The 2D fluid model used in this study is suitable to simulate its effects for a long time-scale because of much lower calculation costs than the 3D PIC model. However, the 2D fluid model cannot deal with kinetic model effects like sheath effects precisely. In the 2D fluid model, the plasma transport along magnetic field line is modeled by using 1D sheath model as mentioned in Sec. 2.1 phenomenologically in order to consider the sheath effects which can be included naturally in the 3D PIC model.

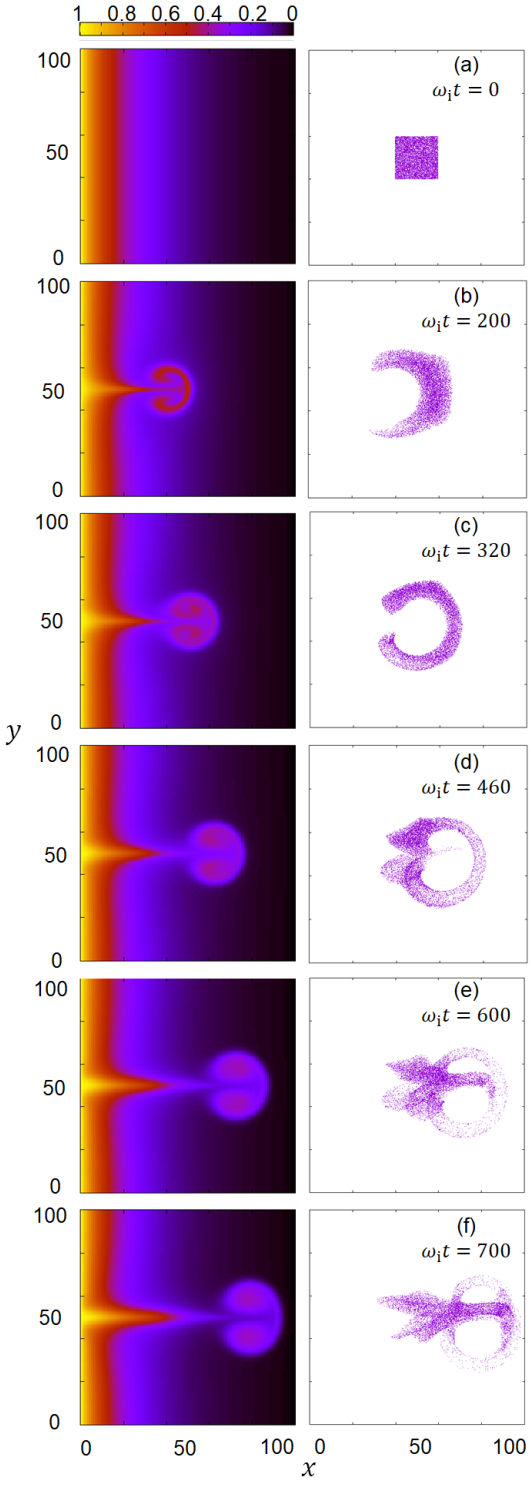

Fig. 6 Initial distribution and simulation results of (left side) plasma density and (right side) impurity ions. These profiles are shown as a snapshot at various time steps, and distributions of plasma density and impurity ions are at the same time steps. Initial distribution of impurity ions is located in the center area of computer simulation domain. Plasma blob penetrates into the impurity region.

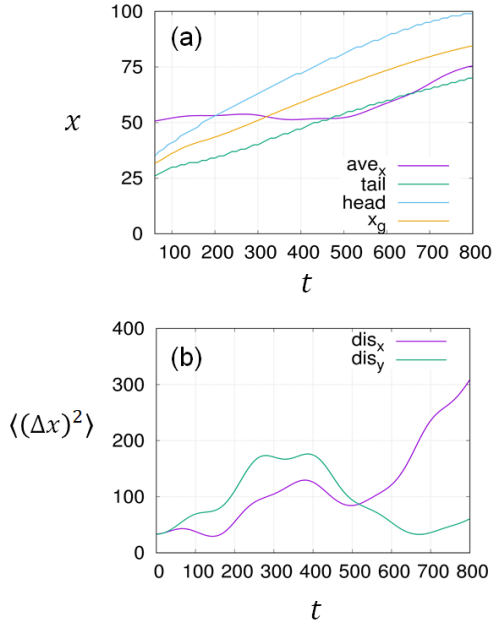

Fig. 7 (a)The time evolution of blob x direction location and impurity ions ensemble mean of position. (b) The time evolution of impurity ions ensemble mean of dispersion.

In this study, we mainly focused on understanding the plasma blob effects on impurity transport for a long time-scale. Thus, we have analyzed its effects by using not the 3D PIC model but the 2D fluid model, because the 2D fluid model is suitable to simulate for a long time-scale as mentioned above.

The results in this study show as follows: 1) the plasma blob effects on impurity transport for a long time-scale was analyzed for the first time, and 2) impurity ions penetrate from plasma blob rear part into the plasma blob inside and transport radially outwards with plasma blob transport in a long time-scale simulation. 2) is the new tendency compared to the results in Ref. [9].

As mentioned above, the present fluid model and results are based on the assumptions and simplifications. Therefore, it will be necessary to analyze the effects of plasma blob on impurity transport the for a long time-scale as much as possible by using 3D PIC model.

In this simulation, the impurity ions Larmor radius ρ_{imp} is given by $\rho_{\mathrm{imp}} = v/\Omega_{\mathrm{imp}}$, v is the initial impurity ions speed and Ω_{imp} is the impurity ions cyclotron frequency. The blob size δ_{blob} is $\delta_{\mathrm{blob}} \sim 20\rho_s$. Comparing the ρ_{imp} with ρ_s and δ_{blob}, we get the rates as follows: $\rho_{\mathrm{imp}}/\rho_s \sim 2.74$ and $\rho_{\mathrm{imp}}/\delta_{\mathrm{blob}} \sim 0.137$. The impurity ions Larmor radius is sufficiently smaller than the plasma blob size. At least for this impurity ions Larmor radius, the impurity ions transport is strongly influenced by the plasma blob transport as mentioned above. Moreover, this motion of the impurity ions seems like eddy motion. We have to study a relation between this eddy motion of impurity ions and the plasma blob motion. That is our future work.

Figure 7 (a) shows the time evolutions of the plasma blob location and impurity ions ensemble mean of position. The term ave_x represents the impurity ions mean position

in the x direction. The terms tail, head, and x_g represent the plasma blob max x position, plasma blob min x position, and center of gravity of the plasma blob in the x direction, respectively. In order to calculate the terms tail, head and x_g, following steps are done; 1) when the difference between $n_x(t)$ and $n_x(0)$ is larger than zero: $n_x(t) - n_x(0) > 0$, the min x position is the tail, where $n_x(t)$ is the x-direction plasma density averaged in the y direction at 'timestep'= t and $n_x(0)$ is the x-direction initial plasma density averaged in the y direction, 2) when the rate between $n_x(t)$ and $n_x(0)$ is larger than two in the range of 'tail' $\leq$ 100: $n_x(t)/n_x(0) > 2$, the max x position is the head, and 3) the x_g is calculated in the range of 'tail' $\leq x \leq$ 'head'. The ave_x start decreasing when the head almost reaches the ave_x. The ave_x start increasing when the tail almost reaches the ave_x. This mechanism is explained as follows: 1) the plasma blob sweeps the impurity ions when the plasma blob reaches the impurity ions region, 2) the impurity ions are transported radially towards the Separatrix by the $\mathbf{E} \times \mathbf{B}$ drift around the blob, 3) after the plasma blob completely penetrates the impurity region, the impurity ions become to be transported into the plasma blob by the $\mathbf{E} \times \mathbf{B}$ drift inside the plasma blob, and 4) the impurity ions are transported with the plasma blob radially outward transport. The step 2) and 4) reflect the decreasing ave_x and increasing ave_x, respectively. Figure 7 (b) shows the time evolution of the impurity ions ensemble mean of dispersion. The terms dis_x and dis_y represent the impurity ions ensemble mean of dispersion in the x and y direction, respectively. There is a proportional relation between the dis_x and time. This implies that the impurity ions radially transport is diffusion phenomena on the basis of Brownian motion theory [18]. By the way, we have tried to compare the impurity ions velocity with the blob velocity in simulation timestep $t = 500 \sim 700$. These results are as follows: $v_{\text{tail}} = 3.82 \times 10^3$ m/s, $v_{x_g} = 4.51 \times 10^3$ m/s, $v_{\text{head}} = 4.86 \times 10^3$ m/s, $v_{\text{ave}_x} = 5.34 \times 10^3$ m/s, and $v_{\text{dis}_x} = 4.27 \times 10^3$ m/s. The impurity ions velocity is the same order of the plasma blob velocity. The impurity ions are probably transported according to the plasma blob transportation velocity. Therefore, there is a possibility of convection phenomena on the impurity ions transport with plasma blob.

4. Summary and Future Work

In this paper, we have simulated the plasma blob formation and transport by using the 2D interchange turbulence model with the plasma transport along the magnetic field line. Also, the effects of the plasma blob on the impurity ions transport have been studied by using test particle model.

As mentioned in Sec. 3.1, the plasma transport direction is changed due to the plasma transport along magnetic field line. The plasma blob transport direction is $+x$ (= radial outward) and $-y$ (= poloidal) direction. In Sec. 3.2, impurity ions penetrate from plasma blob rear part into the plasma blob inside and transport radially outward with the plasma blob transport in a long time-scale simulation. The velocity of impurity ions is the same order to the plasma blob transport velocity. There is a possibility of diffusion and (/or) convection. Moreover, the motions of impurity ions look like an eddy. In order to understand the effects of the plasma blob on the impurity ions transport, we have to study the impurity ions motion like an eddy in detail. After this work, we will start a parametric sensitivity study, because the impurity ions distribution may possibly change in case the impurity ions Larmor radius is larger than the plasma blob size. In the parametric sensitivity study, we will change the parameters in the wide range; 1) background plasma parameters (plasma potential fluctuation and electron temperature), 2) blob parameters (blob size and speed), and 3) impurity parameters (impurity ions species, valence of impurity ions and initial velocity) to investigate the effects of plasma blob on the impurity transport more precisely. In various situation, the effects of the plasma blob on the impurity ions transport is evaluated quantitatively.

Acknowledgments

This work is performed with the support and under the auspices of the NIFS Collaborative Research Program (NIFS16KNTT038).

[1] S.I. Krasheninnikov *et al.*, J. Plasma Phys. **74**, 679 (2008).
[2] S.I. Krasheninnikov, Phys. Lett. A **283**, 368 (2001).
[3] S.I. Krasheninnikov *et al.*, Nucl. Fusion **57**, 102010 (2017).
[4] G.Q. Yu *et al.*, Phys. Plasmas **10**, 4413 (2003).
[5] J.R. Myra *et al.*, Phys. Plasmas **11**, 4267 (2004).
[6] N. Ohno, J. Plasma Fusion Res. **82**, 205 (2006).
[7] M.V. Umansky *et al.*, Phys. Plasmas **5**, 3373 (1998).
[8] J.A. Boedo *et al.*, Phys. Plasmas **10**, 1670 (2003).
[9] H. Hasegawa *et al.*, Nucl. Fusion **57**, 116008 (2017).
[10] S. Ishiguro *et al.*, J. Plasma Phys. **72**, 1233 (2006).
[11] H. Hasegawa *et al.*, Plasma Fusion Res. **7**, 2401060 (2012).
[12] H. Hasegawa *et al.*, Phys. Plasmas **22**, 102113 (2015).
[13] T. Maeda *et al.*, Contrib. Plasma Phys. **58**, 505 (2018).
[14] N. Bisai *et al.*, Phys. Plasmas **11**, 4018 (2004).
[15] N. Bisai *et al.*, Phys. Plasmas **12**, 102515 (2005).
[16] S. Sugita *et al.*, Theor. Appl. Mech. Jpn. **57**, 207 (2009).
[17] S. Yamoto *et al.*, Nucl. Fusion **57**, 116051 (2017).
[18] A. Einstein, Annalen der Physik **17**, 549 (1905).